Investigation of the binding of ceramide and palmitoyl-CoA to murine t-ACBP using heteronuclear NMR spectroscopy

J. Onyemata[a], M. Meyer[b], J.M. McKenzie[c], D.J.G. Rees[a] and D.J.R. Pugh[a]*

Murine t-ACBP is a member of the family of acyl-CoA binding proteins expressed specifically in testis. Acyl-CoA binding proteins (ACBPs, also know as 'diazepam binding inhibitors' or 'DBIs') bind long-chain acyl-CoA esters with high affinity and act as intracellular transporters and pool formers for acyl-CoA. They are also endogenous ligands for the peripheral benzodiazepine receptor (PBR), which is localized in the mitochondrial membrane, and is thought to regulate the opening of the permeability transition pore complex (PTPC), a central event in apoptosis. We have shown previously that knock-out of t-ACBP leads to resistance to ceramide-induced apoptosis in Chinese hamster ovary (CHO) cells. We have also shown that transduction of recombinantly-produced t-ACBP into CHO cells leads to apoptosis by activation of caspase 3. One possible explanation for this behaviour is that ceramide up-regulates the interaction of t-ACBP with the PBR, leading to opening of the PTPC. A second explanation is that knock-out of t-ACBP leads to reduction in the availability of palmitoyl-CoA, and consequently to a lowering of the level of endogenous ceramide, rendering the cells less sensitive to exogenously introduced ceramide. We have recombinantly expressed ^{13}C- and ^{15}N-enriched samples of murine t-ACBP and used heteronuclear NMR spectroscopy to show that it binds strongly to palmitoyl-CoA. No significant binding was observed to either C_2-ceramide or C_{16}-ceramide. We conclude from this that if t-ACBP does play a role in the opening of the PTPC in response to ceramide, it does not do so by direct interaction with ceramide. We therefore conclude that it is the interaction of t-ACBP with palmitoyl-CoA that holds the key to its role in ceramide-induced apoptosis. This preliminary study serves to illustrate the power of NMR spectroscopy as a tool for probing protein–ligand and protein–protein interactions, which has not previously been exploited in South Africa.

Introduction

The apoptosis-inducing potential of the sphingolipid ceramide is well known,[1] yet the exact mechanism is still poorly understood. In an attempt to identify proteins involved in ceramide-induced apoptosis, we screened retrovirally-mutagenized Chinese hamster ovary (CHO) cells for cells resistant to C_2-ceramide-induced apoptosis.[2] One of the cell lines identified contained an insertion into the promoter region of the gene coding for the testis-specific isoform of acyl-CoA (t-ACBP) (NM_021294; NP_067269; mouse protein O09035). Antibodies were raised against recombinantly-produced protein, which showed that in CHO cells t-ACBP localizes to the mitochondria, which is consistent with what has been observed for other ACBP proteins.[3, 4] Whether the antibodies are specific for t-ACBP, as opposed to other members of the family, has not been determined. We have shown subsequently that transduction of recombinantly-produced t-ACBP protein into CHO cells leads to apoptosis by activation of caspase 3 (M. Meyer *et al.,* manuscript in preparation).

t-ACBP is an 87-residue mouse protein belonging to the acyl-CoA-binding protein family (ACBP), and sharing 54% amino acid sequence identity with bovine liver acyl-CoA-binding protein. ACBP proteins bind long-chain (C_{14}–C_{22}) acyl-CoA esters with nanomolar affinity.[5,6] The ACBP family can be sub-divided into a number of groups on the basis of primary sequence: l-ACBP, which is expressed in all tissue types and appears to play a role in acyl-CoA metabolism; b-ACBP, which is expressed predominantly in brain; t-ACBP, which is also known as 'endozepine' or 'endozepine-like peptide', is expressed predominantly in testis and appears to play a role in spermatogenesis;[7–9] and m-ACBP, which forms part of larger proteins which may be membrane associated. Although t-ACBP does not appear to be expressed in primates,[10] it is expressed in rat testis[7–9] and in Chinese hamster ovary cells, where it is found predominantly in mitochondria.[2] There is some confusion in the literature as to the use of the name 'endozepine': although in early works it was used to refer to the whole class of ACBP/DBI proteins,[11–14] more recently it has come to be used to denote the testis-specific form of ACBP.[7–10,15] However, there is also a wide literature on 'endogenous benzodiazepine-like compounds' (see, for example, ref. 16), which are also called 'endozepines' and should not be confused with acyl-CoA binding proteins.

Acyl-CoA binding proteins were initially identified as neuropeptides which inhibited binding of diazepam to the benzodiazepine-binding site on the $GABA_A$ receptor,[14,17] giving rise to the alternative name 'diazepine binding inhibitors' or 'DBIs'.[18,19] However, their ability to function as neuropeptides remains to be verified.[6] In the meantime, ACBPs have been shown to play a role in a wide range of cellular functions, including fatty chain elongation, protein sorting and vesicular trafficking.[20] ACBPs are included among a number of proteins released from mitochondria following opening of the mitochondrial permeability transition pore complex (PTPC) during apoptosis.[21,22] While the observed protein is described in ref. 21 as 'endozepine', it is clear from the data that it is l-ACPB, rather than t-ACBP, to which they are referring. Ligation of the mitochondrial (peripheral) benzodiazepine receptor (PBR), which is localized in the mitochondrial membrane,[23] has been shown to lead to opening of the PTPC.[24] Since ACBPs also bind to the PBR,[25–27] it is possible that ACBPs are involved in regulating the opening of the PTPC during apoptosis. In that case, a possible explanation for the enabling effect of t-ACBP on ceramide-induced apoptosis is that ceramide directly modulates the interaction of t-ACBP with the PBR, leading to opening of the PTPC.

[a]Department of Biotechnology, University of the Western Cape, Private Bag X17, Bellville 7535, South Africa.
[b]National Centre for Biomedical Engineering Science, National University of Ireland, Galway, Ireland.
[c]NMR Laboratory, Central Analytical Facility, University of Stellenbosch, Private Bag X1, Matieland 7602, South Africa.
*Author for correspondence. E-mail: dpugh@uwc.ac.za

In addition to their interaction with the PBR, ACBPs have been well described as acyl-CoA binding proteins.[28] ACBPs play the role of acyl-CoA transporters and pool-formers, maintaining a supply of soluble acyl-CoAs for a wide range of cellular processes.[5,19,29–32] These include endogenous synthesis of ceramide by serine palmitoyl-CoA transferase, for which palmitoyl-CoA is a substrate.[33] An alternative explanation for the effect of t-ACBP knock-out on ceramide-induced apoptosis is that disruption of the pool-forming activity of t-ACBP may lead to suppression of endogenous levels of ceramide, resulting in reduced sensitivity to exogenously introduced ceramide.

Previous structural studies have investigated the interactions between members of the ACBP family and a range of different-chain-length acyl-CoAs.[34] The structure of bovine l-ACBP bound to palmitoyl-CoA has been determined using heteronuclear NMR,[35] and the residues involved in the interaction identified using ^{15}N-HSQC spectra. The molecule has been used extensively as a model system to study the folding and stability of alpha-helical proteins[36–40] using NMR spectroscopy. The structures of l-ACBP from bovine liver and from P. falciparum have been determined using X-ray crystallography,[41] and a number of differences observed between the binding pockets of the two proteins, which correlate with small changes in specificity. Although no previous structural studies have been reported on t-ACBP, due to the high degree of sequence similarity its structure is not expected to be significantly different from that of l-ACBP. However, the presence of 20 highly conserved residues specific to the t-ACBP sub-family[6] suggests that there may be significant functional differences between t-ACBPs and other members of the ACBP family.

We have addressed two possible explanations for the effect of the knock-out of t-ACBP on ceramide-induced apoptosis. First, that t-ACBP interacts directly with ceramide, abolishing its interaction with the peripheral benzodiazapine receptor, and thereby preventing opening of the mitochondrial transition pore. Second, that t-ACBP plays a role in the maintenance of intracellular levels of endogenous ceramide by supplying palmitoyl-CoA to the biosynthetic ceramide pathway. Knock-out of t-ACBP would therefore be expected to lead to a lowering of endogenous ceramide levels, thereby rendering the cells less sensitive to exogenously introduced ceramide.

Materials and methods

Sequences

The nucleotide sequence coding for t-ACBP was PCR amplified out of genomic DNA isolated from mouse embryonic stem cell using forward primer 5′CATGCTAGATCTATGAGCCAAGTG3′ and reverse primer 5′GAAGACCTCGAGTTAGCATGGCTC3′. Primers were designed based on the gene sequence AF229807. The forward primer incorporated a *Bg*l II site and the reverse an *Xho* I site for cloning into the *Bam* HI and *Xho* I sites in the multiple cloning cassette of the pGEX-6P-2 vector.

Protein expression and purification

Transformed cells were grown at 37°C in M9 Minimal Medium (incorporating $^{15}NH_4Cl$ and supplemented with 2 g/l ^{13}C-glucose) until the OD_{260} reached 0.4–0.6, after which they were induced with 1 mM IPTG and grown for a further 16–18 hours at 30°C. The cells were harvested and re-suspended in GST Binding Buffer (PBS, pH 7.4, including 150 mM NaCl, 0.01% Triton, 1 mM DTT, 1 mM EDTA, 1 mM PMSF), after which they were lysed using the freeze–thaw method (–80°C for 5 min followed by 37°C for 5 min, repeated 3 times). Following centrifugation (6000 × g for 30 min at 4°C) the supernatant was loaded onto a 10 ml gravity-fed glutathione–agarose column and the column washed with 3 column volumes of binding buffer. The fusion protein was eluted with elution buffer (50 mM Tris-HCl, pH 8, including 15 mM reduced glutathione, 1 mM EDTA, 1 mM PMSF).

Eluted fusion protein was first dialysed into cleavage buffer (50 mM Tris-HCl, pH 7.0, including 150 mM NaCl, 1 mM EDTA, 1 mM DTT, 0.01% Triton, 1 mM PMSF) and then 3C protease was added (home-made, activity un-characterized) and cleavage allowed to take place at 4°C overnight. Cleaved GST was removed using 20 HQ anion exchange chromatography; at pH 7 the GST (pI 5.6) was retained by the column whereas the target protein (pI 8.8) remained behind in the flow-through. As a final purification step, the target protein was concentrated into 1 ml using YM-3 Centriprep devices (Millipore, Bedford, MA) and applied to a 1 m × 0.8 cm^2 Sephacryl S100 size exclusion column (Amersham Biosciences), which had been equilibrated in NMR Buffer (50 mM sodium phosphate, pH 6.0, + 10 mM DTT + 50 mM NaCl + 7% D_2O). Fractions containing t-ACBP were pooled and concentrated into 500 μl for NMR analysis. Mass spectrometry showed a single species of the expected molecular weight. The concentration was quantified using Bradford Assay,[45] using commercial lysozyme as a reference.

NMR

All NMR spectra were recorded on the 600-MHz Varian NMR spectrometer of the Central Analytical Facility at the University of Stellenbosch. Spectra were processed using NMRPIpe[46] and visualized using NMRView.[47] ^{15}N-HSQC spectra were recorded using a 5 mm indirect detection PFG probe, using the ghsqc_da pulse sequence, with 8 transients per FID, 128 increments in the indirect dimension and 1024 complex points in the direct dimension.

For sequential assignment, CBCA(CO)NH and HNCACB spectra (refs 42 and 50) were recorded using a 5 mm HCN PFG triple-resonance probe, using pulse-sequences from the Varian BioPack software suite (Varian, Inc., Palo Alto, CA); 8 transients per FID, 128 increments in the carbon dimension and 64 increments in the nitrogen dimension were used in both cases. Strip plots were generated in NMRView using a peak list picked from an HNCO spectrum. Assignments were checked with the help of an H(CCO)NH spectrum, which correlates side-chain protons of residue $i-1$ with the H^N and N of residue i.

Binding analysis

Peak volumes were calculated using NMRView, and corrected for changes in concentration due to changes in the volume of the NMR sample on addition of ligand. θ was calculated using Equation (1). Binding curves were generated using proFit (QuantumSoft, Zürich, Switzerland; www.quansoft.com) and fitted to the theoretical expression

$$\theta = \frac{[P] + [L] + K_D - \sqrt{([P] + [L] + K_D)^2 - 4[P][L]}}{2[P]}, \quad (1)$$

where $[P]$ is the protein concentration (fixed), $[L]$ is the ligand concentration (the independent variable) and K_D is the dissociation constant whose value is to be determined. $[P]$ and K_D were both allowed to vary during the fitting.

Modelling

A model of t-ACBP was generated using MODELLER[48,49] (accessible through the ESyPred3D server: www.fundp.ac.be/urbm/bioinfo/esypred) based its primary sequence homology with l-ACBP. Graphical representations were generated using PyMOL [DeLano W.L. (2002). The PyMOL Molecular Graphics System. DeLano Scientific, San Carlos, CA; www.pymol.org].

Results

To investigate the binding of various ligands to t-ACBP, ^{15}N-enriched samples of GST-tagged t-ACBP were expressed in bacteria by growing transformed *E. coli* cells on minimal media incorporating [^{15}N]ammonium chloride as the sole nitrogen source. The protein was expressed as a C-terminal fusion with the 26-kDa glutathione-S-transferase (GST) protein from *S. japonicum*, and the GST was subsequently removed using 3C protease followed by anion exchange chromatography. Removal of GST left the five amino acids Gly-Pro-Leu-Gly-Ser fused to the N-terminus of t-ACBP, resulting in a 92-residue protein with an expected size of 10.2 kDa. After final purification using size exclusion chromatography, the protein was concentrated to a final concentration of 0.5 mM for NMR analysis. A 1-dimensional proton NMR spectrum is shown in Fig. 1.

Two-dimensional ^{15}N-HSQC NMR spectra were used to probe the binding of ligands to ^{15}N-enriched t-ACBP. Each resonance in a ^{15}N-HSQC spectrum of a protein (with a number of exceptions, including the NH_2 doublets at the top right of the spectrum) corresponds to the backbone NH group of a single amino acid, with the horizontal and vertical coordinates corresponding to the magnetic precession frequencies of the ^{1}H and ^{15}N nuclei, respectively. Both frequencies are highly sensitive to the binding of ligands in the immediate vicinity of the NH group, often due to the making or breaking of hydrogen bonds involving the NH group, making it a powerful probe of protein–ligand, as well as of protein–protein, interactions.

Addition of C_{16}-ceramide had no effect on the ^{15}N-HSQC spectrum, even at fivefold excess relative to the protein concentration. Similar results were obtained using C_2-ceramide. We conclude from this that there is no significant binding of either form of ceramide to t-ACBP. In contrast, addition of even small amounts of palmitoyl-CoA led to a decrease in the amplitude of a number of resonances, and the appearance of new resonances nearby. Figure 2 shows an overlay of t-ACBP before (in black) and after (in red) the addition of a twofold excess of palmitoyl-CoA. A large number of the black resonances have completely disappeared, suggesting that at twofold excess the protein is already completely saturated. We conclude from the changes to the spectrum that palmitoyl-CoA binds directly and strongly to t-ACBP. Only ^{15}N-enriched compounds were visible in ^{15}N-HSQC spectra, which means that the ligand itself did not appear in the spectrum. In total we identified 20 resonances which disappeared from the spectrum on addition of ligand, with the appearance of a similar number elsewhere; however, until both the liganded and the un-liganded spectra have been assigned, we are not able to match the liganded with the un-liganded resonances. Two cases in which both the un-liganded and the corresponding liganded resonances are clearly identifiable are indicated by boxes.

Furthermore, since the liganded and un-liganded states have distinct resonances, we conclude that we are in the so-called 'strong-binding limit'. In this case the liganded and un-liganded states behave as separate species during the NMR acquisition period, and the respective resonances are proportional to the numbers of molecules in each state. (This is in contrast to the 'weak-binding limit', in which the liganded and un-liganded states inter-convert during the acquisition time, and a single resonance is observed at the population-weighted average of the two resonances.)

Since we were in the strong-binding limit, the bound fraction θ can be expressed as

$$\theta = \frac{V_{\text{bound}}}{V_{\text{bound}} + V_{\text{unbound}}}, \qquad (2)$$

where V_{bound} and V_{unbound} represent the volumes of the respective resonances. Figure 3B shows a plot of θ as a function of ligand concentration for residue Lys[17], which is one of the residues indicated by a box in Fig. 2. θ increases approximately linearly with ligand concentration and levels off sharply at $\theta = 1$, when the ligand concentration equals the protein concentration.

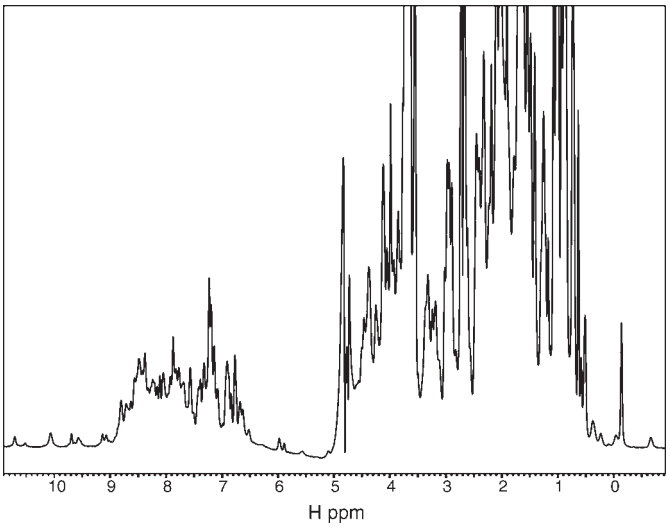

Fig. 1. One-dimensional proton NMR spectrum of t-ACBP, recorded in 93% H_2O/7% D_2O at 25°C on the 600-MHz Varian NMR spectrometer at the University of Stellenbosch. The concentration of the sample was 1.2 mM. The residual H_2O resonance is at 4.7 ppm and the backbone H^N resonances which form the focus of NMR-based binding experiments are found between 7 and 11 ppm. The spectrum is well dispersed (note in particular the peaks to the right of 0 ppm and to the left of 9 ppm), indicating that the protein is folded.

This indicates that the protein sequesters all available ligand until it is saturated, which corresponds to strong binding. The solid line in Fig. 3B corresponds to the theoretical expression for θ [Equation (1)], and gives a value for the dissociation constant K_D of 3.6 ± 6.9 μM. K_D is therefore in the micromolar range, corresponding to strong binding. However, as can be seen from the error bars, the value obtained was an upper limit on K_D, since decreasing K_D further would have the effect of only sharpening the 'turnover' of the graph in Fig. 3B, and our data are not comprehensive enough to probe this area of the curve. A more significant measurement of K_D would require the protein concentration to be of the same order of magnitude as K_D. This

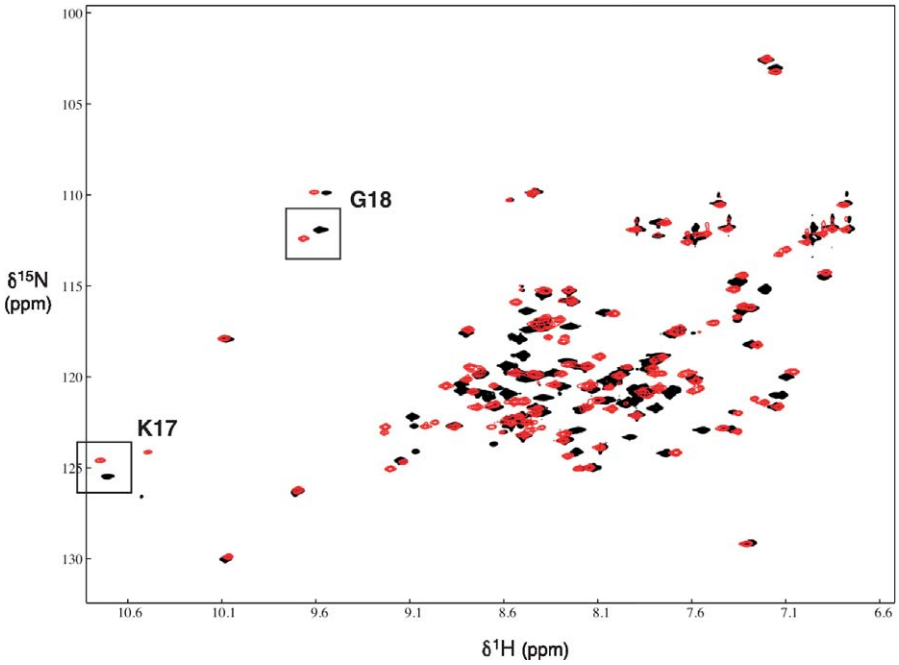

Fig. 2. Overlay of the ^{15}N-HSQC spectrum of t-ACBP before (in black) and after (in red) addition of twofold excess palmitoyl-CoA. In a large number of cases the black resonances have completely disappeared from the liganded spectrum, indicating that at twofold excess the protein is already completely saturated. Two well-resolved examples of liganded/un-liganded pairs of resonances are indicated by boxes.

would not, however, be measurable using this method, since a micromolar protein concentration would be difficult to detect using NMR.

To establish the identities of the amino acids corresponding to the shifting resonances, double-labelled (^{13}C- and ^{15}N-enriched) samples of t-ACBP were prepared and used to record triple-resonance coherence transfer spectra from which we sequentially assigned 80% of the residues (refs 42 and 50). Assignment of the protein is ongoing and a more complete treatment of the assignments will be published elsewhere. Based on these assignments, we have established that the two resonances boxed in Fig. 2 correspond to Lys^{17} and Gly^{18}, respectively.

To determine if the residues identified above are consistent with the binding site identified in previous studies, we used MODELLER to build an homology model of t-ACBP based on the structure of bovine l-ACBP. Figure 4A shows a surface representation of the modelled structure of t-ACBP, with Lys^{17} and Gly^{18} indicated in red. Figure 4B shows the same view of the NMR structure of bovine l-ACBP, with palmitoyl-CoA shown in green.

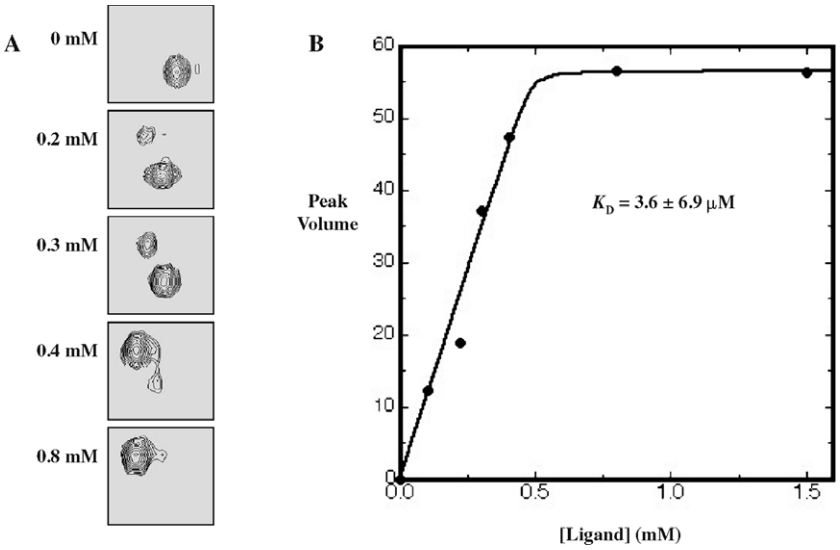

Fig. 3. **A**, Close-up of the region around Lys^{17} showing the un-liganded resonance (bottom right) being replaced by the liganded resonance (top left) as ligand is added; **B**, plot of the volume of the liganded peak as a function of ligand concentration. The fitted curve corresponds to Equation (1).

It is clear by comparison of Figs 4A and B that palmitoyl-CoA binds into a similarly shaped binding pocket on t-ACBP and that the residues identified by NMR are likely to be intimately involved in the binding interaction. Perhaps interestingly, a 10-residue stretch of the protein which we have so far not been able to assign due to low intensity of the resonances, lies directly in the modelled binding pocket. The reason for the low intensity is not clear, although it is possible that the sample contains acyl-CoA-like molecules originating from the expression host which are engaging in on–off interactions, leading to exchange-broadening of the NMR resonances.

Discussion

We have previously shown that CHO cells in which the murine t-ACBP protein has been knocked out are resistant to ceramide-induced apoptosis, and that transduction of recombinantly-produced protein into CHO cells results in apoptosis by the induction of caspase 3.[2] Given that t-ACBP is a member of the acyl-CoA-binding protein family, we sought to determine whether t-ACBP exerts its effect on apoptosis directly, by interacting with ceramide, or indirectly, by acting as a transporter of palmitoyl CoA.

We have expressed murine t-ACBP protein recombinantly in *E. coli* and used heteronuclear NMR to show that it does not have any significant interaction with either C_2-ceramide or C_{16}-ceramide. If t-ACBP does play a role in permeabilization of the mitochondrial membrane in response to ceramide, it does not do so by direct interaction with ceramide. On the other hand, it does interact strongly with palmitoyl-CoA, with a K_D in the sub-micromolar range.

Using double-labelled samples, we sequentially assigned the protein using triple-resonance transfer experiments, and hence identified a number of residues involved in the binding interaction between t-ACBP and palmitoyl-CoA. These experiments were carried out on the 600-MHz Varian NMR spectrometer at the University of Stellenbosch, and represent the first sequential assignment of a protein NMR spectrum in South Africa. The binding residues identified by NMR are consistent with the homology model of t-ACBP based on the structure of l-ACBP bound to palmitoyl-CoA. In future work, we aim to produce mutants by substitution of the binding residues in order to abolish binding to palmitoyl-CoA while retaining the structural integrity of the overall protein. These mutants will then be tested

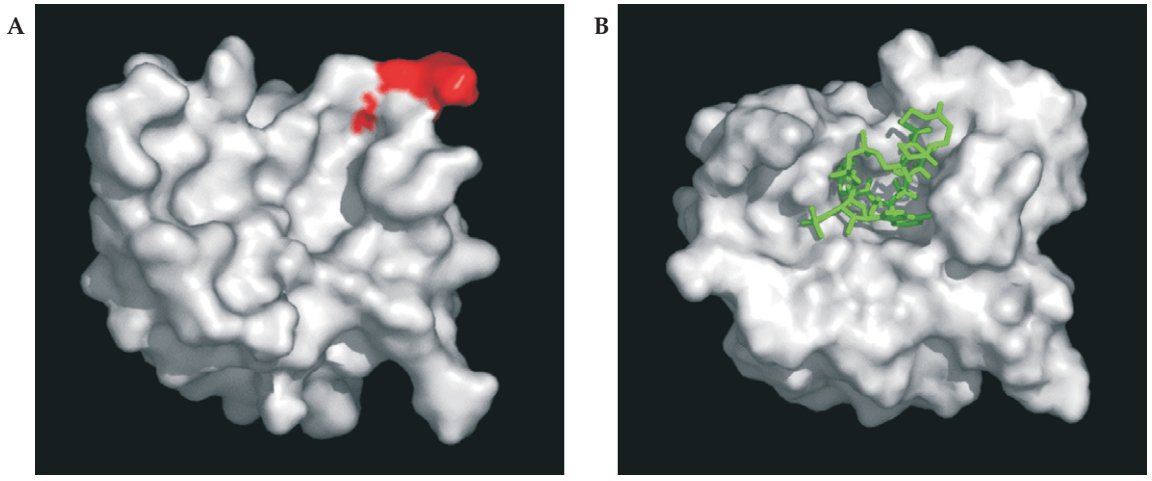

Fig. 4. **A**, Surface representation of the modelled structure of t-ACBP, showing the boxed residues from Fig. 2 in red; **B**, surface representation of the same orientation of l-ACBP, showing palmitoyl-CoA bound in green.

for their ability to induce apoptosis in order to test the hypothesis that transport of palmitoyl-CoA by t-ACBP is required for ceramide-induced apoptosis.

The preliminary results reported here illustrate the power of heteronuclear NMR spectroscopy as a tool for investigating protein–ligand and protein–protein interactions. ^{15}N-HSQC spectra such as the one shown in Fig. 2 require only moderate concentrations of protein (>0.1 mM in a sample volume of 0.5 ml) and require that the samples be ^{15}N-labelled but not ^{13}C-labelled. For protein–protein interactions, one of the proteins should be ^{15}N-labelled and the other unlabelled, so that only the resonances of the labelled protein appear in the ^{15}N-HSQC spectrum. Experiments of this type provide a convenient method of screening a single protein against a library of potential ligands which is currently in widespread use in the pharmaceutical industry.[43,44] If binding is observed, residues involved in the binding site may be identified by expressing ^{13}C-labelled samples and using triple-resonance experiments to assign sequentially the resonances of the ^{15}N-HSQC spectrum, as described elsewhere in this issue.[50]

1. Obeid L.M. *et al.* (1993). Programmed cell death induced by ceramide. *Science* **259**, 1769–1771.
2. Meyer M. (2003). Ph.D. thesis, University of the Western Cape, Bellville.
3. Papadopoulos V. *et al.* (1991). Diazepam binding inhibitor and its processing products stimulate mitochondrial steroid biosynthesis via an interaction with mitochondrial benzodiazepine receptors. *Endocrinology* **129**(3), 1481–1488.
4. Li H.Y. and Chye M.L. (2003). Membrane localization of *Arabidopsis* acyl-CoA binding protein ACBP2. *Plant Mol. Biol.* **51**(4), 483–492.
5. Kragelund B.B., Knudsen J. and Poulsen F.M. (1999). Acyl-coenzyme A binding protein (ACBP). *Biochim. Biophys. Acta* **1441**(2–3), 150–161.
6. Burton M. *et al.* (2005). Evolution of the acyl-CoA binding protein (ACBP). *Biochem J.* **392**(Pt 2), 299–307.
7. Pusch W. *et al.* (1999). Rat endozepine-like peptide (ELP): cDNA cloning, genomic organization and tissue-specific expression. *Gene* **235**(1–2), 51–57.
8. Valentin M. *et al.* (2000). Structure and expression of the mouse gene encoding the endozepine-like peptide from haploid male germ cells. *Eur. J. Biochem.* **267**(17), 5438–5449.
9. Pusch W. *et al.* (2000). The rat endozepine-like peptide gene is highly expressed in late haploid stages of male germ cell development. *Biol. Reprod.* **63**(3), 763–768.
10. Ivell R. *et al.* (2000). Progressive inactivation of the haploid expressed gene for the sperm-specific endozepine-like peptide (ELP) through primate evolution. *Gene* **255**(2), 335–345.
11. Todaro G.J., Rose T.M. and Shoyab M. (1991). Human DBI (endozepine): relationship to a homologous membrane associated protein (MA-DBI). *Neuropharmacology* **30**(12B), 1373–1380.
12. Rose T.M., E.R. Schultz E.R. and G.J. Todaro G.J. (1992). Molecular cloning of the gene for the yeast homolog (ACB) of diazepam binding inhibitor/endozepine/acyl-CoA-binding protein. *Proc. Natl Acad. Sci. USA* **89**(23), 11287–11291.
13. Marquardt H., Todaro G.J. and Shoyab M. (1986). Complete amino acid sequences of bovine and human endozepines. Homology with rat diazepam binding inhibitor. *J. Biol. Chem.* 261(21), 9727–9731.
14. Shoyab M. *et al.* (1986). Isolation and characterization of a putative endogenous benzodiazepineoid (endozepine) from bovine and human brain. *J. Biol. Chem.* **261**(26), 11968–11973.
15. Pusch W. *et al.* (1996). A novel endozepine-like peptide (ELP) is exclusively expressed in male germ cells. *Mol. Cell Endocrinol.* **122**(1), 69–80.
16. Cortelli P. *et al.* (2005). Endozepines in recurrent stupor. *Sleep Med. Rev.* **9**(6), 477–487.
17. Guidotti A. *et al.* (1983). Isolation, characterization, and purification to homogeneity of an endogenous polypeptide with agonistic action on benzodiazepine receptors. *Proc. Natl Acad. Sci. USA* **80**(11), 3531–3535.
18. Knudsen J. (1991). Acyl-CoA-binding and transport, an alternative function for diazepam binding inhibitor (DBI), which is identical with acyl-CoA-binding protein. *Neuropharmacology* **30**(12B), 1405–1410.
19. Knudsen J. *et al.* (1993). The function of acyl-CoA-binding protein (ACBP)/diazepam binding inhibitor (DBI). *Mol. Cell Biochem.* **123**(1–2), 129–138.
20. Faergeman N.J. *et al.* (2004). Acyl-CoA-binding protein, Acb1p, is required for normal vacuole function and ceramide synthesis in *Saccharomyces cerevisiae*. *Biochem. J.* **380**(Pt 3), 907–918.
21. Patterson S.D. *et al.* (2000). Mass spectrometric identification of proteins released from mitochondria undergoing permeability transition. *Cell Death Differ.* **7**(2), 137–144.
22. Van Loo G. *et al.* (2002). A matrix-assisted laser desorption ionization post-source decay (MALDI-PSD) analysis of proteins released from isolated liver mitochondria treated with recombinant truncated Bid. *Cell Death Differ.* **9**(3), 301–308.
23. Woods M.J., Zisterer D.M. and Williams D.C. (1996). Two cellular and subcellular locations for the peripheral-type benzodiazepine receptor in rat liver. *Biochem Pharmacol.* **51**(10), 1283–1292.
24. Hirsch T. *et al.* (1998). PK11195, a ligand of the mitochondrial benzodiazepine receptor, facilitates the induction of apoptosis and reverses Bcl-2-mediated cytoprotection. *Exp. Cell Res.* **241**(2), 426–434.
25. Garnier M. *et al.* (1993). Diazepam binding inhibitor is a paracrine/autocrine regulator of Leydig cell proliferation and steroidogenesis: action via peripheral-type benzodiazepine receptor and independent mechanisms. *Endocrinology* **132**(1), 444–458.
26. Papadopoulos V. *et al.* (1997). Peripheral benzodiazepine receptor in cholesterol transport and steroidogenesis. *Steroids* **62**(1), 21–28.
27. Burgi B., Lichtensteiger W. and Schlumpf M. (2000). Diazepam-binding inhibitor/acyl-CoA-binding protein mRNA and peripheral benzodiazepine receptor mRNA in endocrine and immune tissues after prenatal diazepam exposure of male and female rats. *J. Endocrinol.* **166**(1), 163–171.
28. Rosendal J., Ertbjerg P. and Knudsen J. (1993). Characterization of ligand binding to acyl-CoA-binding protein. *Biochem. J.* **290**(Pt 2), 321–326.
29. Rasmussen J.T. *et al.* (1994). Acyl-CoA-binding protein (ACBP) can mediate intermembrane acyl-CoA transport and donate acyl-CoA for beta-oxidation and glycerolipid synthesis. *Biochem. J.* **299**(Pt 1), 165–170.
30. Knudsen J. *et al.* (1994). Yeast acyl-CoA-binding protein: acyl-CoA-binding affinity and effect on intracellular acyl-CoA pool size. *Biochem. J.* **302**(Pt 2), 479–485.
31. Mandrup S. *et al.* (1993). Effect of heterologous expression of acyl-CoA-binding protein on acyl-CoA level and composition in yeast. *Biochem. J.* **290**(Pt 2), 369–374.
32. Huang H. *et al.* (2005). Acyl-coenzyme A binding protein expression alters liver fatty acyl-coenzyme A metabolism. *Biochemistry* **44**(30), 10282–10297.
33. Hojjati M.R., Li Z. and Jiang X.C. (2005). Serine palmitoyl-CoA transferase (SPT) deficiency and sphingolipid levels in mice. *Biochim. Biophys. Acta* **1737**(1), 44–51.
34. Kragelund B.B. *et al.* (1999). Conserved residues and their role in the structure, function, and stability of acyl-coenzyme A binding protein. *Biochemistry* **38**(8), 2386–2394.
35. Kragelund B.B. *et al.* (1993). Three-dimensional structure of the complex between acyl-coenzyme A binding protein and palmitoyl-coenzyme A. *J. Mol. Biol.* **230**(4), 1260–1277.
36. Fieber W., Kristjansdottir S. and Poulsen F.M. (2004). Short-range, long-range and transition state interactions in the denatured state of ACBP from residual dipolar couplings. *J. Mol. Biol.* **339**(5), 1191–1199.
37. Teilum K. *et al.* (2005). Different secondary structure elements as scaffolds for protein folding transition states of two homologous four-helix bundles. *Proteins* **59**(1), 80–90.
38. Kristjansdottir S. *et al.* (2005). Formation of native and non-native interactions in ensembles of denatured ACBP molecules from paramagnetic relaxation enhancement studies. *J. Mol. Biol.* **347**(5), 1053–1062.
39. Lindorff-Larsen K. *et al.* (2004). Determination of an ensemble of structures representing the denatured state of the bovine acyl-coenzyme a binding protein. *J. Am. Chem. Soc.* **126**(10), 3291–3299.
40. Teilum K. *et al.* (2000). Formation of hydrogen bonds precedes the rate-limiting formation of persistent structure in the folding of ACBP. *J. Mol. Biol.* **301**(5), 1307–1314.
41. van Aalten D.M. *et al.* (2001). Binding site differences revealed by crystal structures of *Plasmodium falciparum* and bovine acyl-CoA binding protein. *J. Mol. Biol.* **309**(1), 181–192.
42. Reid D.G. *et al.* (1997). Introduction to the NMR of proteins. *Methods Mol. Biol.* **60**, 1–28.
43. Pellecchia M., Sem D.S. and Wuthrich K. (2002). NMR in drug discovery. *Nat. Rev. Drug Discov.* **1**(3), 211–219.
44. Hajduk P.J. and Burns D.J. (2002). Integration of NMR and high-throughput screening. *Comb. Chem. High Throughput Screen* **5**(8), 613–621.
45. Bradford M.M. (1976). A rapid and sensitive method for the quantitation of microgram quantities of protein utilizing the principle of protein-dye binding. *Anal. Biochem.* **72**, 248–254.
46. Delaglio F. *et al.* (1995). NMRPipe: a multidimensional spectral processing system based on UNIX pipes. *J. Biomol. NMR* **6**(3), 277–293.
47. Johnson B.A. and Blevins R.A. (1994). NMRView: A computer program for the visualization and analysis of NMR data. *J. Biomol. NMR* **4**, 603–614.
48. Sali A. *et al.* (1995). Evaluation of comparative protein modeling by MODELLER. *Proteins* **23**(3), 318–326.
49. Lambert C. *et al.* (2002). ESyPred3D: Prediction of proteins 3D structures. *Bioinformatics* **18**(9), 1250–1256.
50. Pugh D.J.R. (2005). Biomolecular NMR spectroscopy in South Africa: the first five years. *S. Afr. J. Sci.* **101**, 421–429.